LBL-35231
UC-404
Preprint

Lawrence Berkeley Laboratory
UNIVERSITY OF CALIFORNIA

Materials Sciences Division

Submitted to Physical Review Letters

Observation of the Quasiparticle Hall Effect in Superconducting $YBa_2Cu_3O_7$

S. Spielman, B. Parks, J. Orenstein, D.T. Nemeth,
J. Clarke, P. Merchant, and D.J. Lew

February 1994

Prepared for the U.S. Department of Energy under Contract Number DE-AC03-76SF00098

DISCLAIMER

LBL-35231
UC-404

Observation of the Quasiparticle Hall Effect in Superconducting $YBa_2Cu_3O_7$

S. Spielman, Beth Parks, J. Orenstein, D.T. Nemeth,
and John Clarke

Department of Physics
University of California
and
Materials Sciences Division
Lawrence Berkeley Laboratory
University of California
Berkeley, California 94720

Paul Merchant

Hewlett-Packard Laboratories, 3500 Deer Creek Road
Palo Alto, California 94304

D.J. Lew

Department of Applied Physics
Stanford University
Stanford, California 94305

February 1994

This work was supported in part by the NSF Grant No. FD93-04394, the Director, Office of Basic Energy Sciences, of the U.S. Department of Energy under Contract No. DE-AC03-76SF00098, and the AT&T Foundation for instrumentation funding.

Observation of the quasiparticle Hall effect in superconducting $YBa_2Cu_3O_7$

S. Spielman,[1] Beth Parks,[1] J. Orenstein,[1]
D. T. Nemeth,[1] John Clarke,[1] Paul Merchant,[2] D. J. Lew[3]

[1]*Materials Science Division, Lawrence Berkeley Laboratory, and the Department of Physics, University of California, Berkeley, California 94720*

[2]*Hewlett-Packard Laboratories, 3500 Deer Creek Road, Palo Alto, California, 94304*

[3]*Department of Applied Physics, Stanford University, Stanford, California, 94305*

Abstract

Coherent time-domain spectroscopy was used to measure the complex transmission tensor of several $YBa_2Cu_3O_7$ thin films in magnetic fields up to 6 T at temperatures from 10 to 200 K. The complex conductivity tensor was determined from transmission measurements in the frequency range 150-800 GHz without the need for Kramers-Kronig analysis. Both the real and imaginary parts of σ_{xy} were found to peak near 40 K, exceeding their normal state values by more than a factor of 10. This behavior is ascribed to the Hall effect of quasiparticles in the superconducting state.

PACS numbers: 74.25.Nf, 74.25.Ha, 74.72.Bk

Below T_c, quasiparticles in the cuprate superconductors constitute a unique low-dimensional, high-mobility and possibly highly anisotropic electronic system. Quasiparticle dynamics, as revealed through measurements of their conductivity, provide clues to the pairing mechanism and are relevant to potential applications which make use of the high transition temperature. Recent studies of quasiparticle conductivity in the gigahertz through terahertz region of the spectrum have led to important discoveries: the rapid decrease in scattering rate just below T_c [1,2], and evidence for states at low energy [3]. By analogy with other low-dimensional systems, we expect measurements of the *conductivity tensor* in the presence of a magnetic field to be useful. However, the Hall conductivity of quasiparticles below T_c has never been reported experimentally, although predicted theoretically long ago [4]. In this work we report the first measurements of the complex conductivity tensor in $YBa_2Cu_3O_7$ thin films in the frequency range from 150 to 800 GHz, using time-domain methods. We ascribe the off-diagonal component to the Hall, or damped cyclotron, motion of quasiparticles.

Nuss *et al.* [1] first demonstrated the utility of coherent time domain spectroscopy as a probe of the high-frequency conductivity of the cuprate superconductors. They showed that by resolving the time-dependence of an electromagnetic pulse transmitted through a thin film sample, the complex transmission coefficient $t(\omega)$ could be determined over a broad spectral range. In the absence of a magnetic field the transmission coefficients of left and right circularly polarized radiation, $t_{\pm}(\omega)$, are degenerate and are related to the conductivity tensor by

$$t_{\pm}(\omega) = \frac{1}{Z_0 d\,\sigma_{\pm}(\omega) + n + 1} \cdot \frac{4n e^{i\Phi(\omega)}}{n+1}, \qquad (1)$$

where Z_0 is the impedance of free space, d is the film thickness and n is the substrate index. Φ is the frequency dependent phase shift due to propagation through the substrate. Both real and imaginary parts of the conductivity, $\sigma_{\pm}(\omega)$ are obtained simply by inverting Eq. (1). The ability to determine the complex response without Kramers-Kronig transformation is particularly useful in understanding the dynamics of the superconducting state, which is dominated by the imaginary, non-dissipative response of the condensate.

In the presence of a magnetic field oriented perpendicular to the sample plane the degeneracy between left and right circularly polarized radiation is lifted (the Faraday effect). Two transmission measurements, rather than one, are required to characterize the conductivity tensor. Because it is difficult to obtain broadband circularly polarized radiation we work in a cartesian basis, using wire grid linear polarizers to control the polarization state. The nondegeneracy appears as off-diagonal terms in the transmission tensor: $t_{xy} = -t_{yx} = \frac{-i}{2}(t_+ - t_-)$.

The spectrometer we have designed for measurement of the transmission tensor in the presence of a static magnetic field is shown in Fig. 1. The sources and detectors of terahertz radiation are microfabricated photoconductive antennas [5]. A voltage-biased antenna generates a short pulse of terahertz radiation when the photoconductor is excited by an optical pulse from a mode-locked Ti:sapphire laser. Similarly, an antenna connected to a current amplifier detects the field of incoming radiation at the moment it is struck by an optical pulse. The time dependence of the terahertz pulse is recorded by continuously varying the interval between the arrival of optical pulses at the genera-

tor and detector. The amplitude spectrum of the radiation is centered at 200-500 GHz (depending on the antenna geometry) and can contain frequency components out to 1 THz. The radiation is coupled into space with hemispherical silicon lenses and guided through the spectrometer with paraboloidal mirrors.

Several features beyond the original design of Nuss *et al.* are incorporated in the spectrometer to measure the complex Faraday effect. The sample is placed at the center of a split-coil superconducting magnet, with the field oriented along the wavevector of the incident radiation. As shown in Fig. 1, the pulse incident on the cryostat passes through a linear polarizer, the outer and inner windows of the cryostat, the substrate, and then the film. The components of the transmission tensor are selected by orienting the second polarizer either parallel (t_{xx}) or perpendicular (t_{xy}) to the first. The third polarizer at 45° ensures that the polarization state of the pulse finally reaching the detector is not affected by the orientation of the analyzing polarizer. Although the source and detector are highly polarized themselves, the first and third wire grid polarizers were added to create a more pure and controllable polarization state.

Achieving the optimum sensitivity to t_{xy} requires that the throughput with crossed polarizers be minimized. The amplitude extinction ratio of two wire grid polarizers alone is about 100 (10^4 in intensity). In the experimental configuration, birefringence in the cryostat windows and substrate limit the extinction ratio. The effect of windows is mitigated by using materials with low birefringence – 0.1 mm Mylar outer windows and fused quartz 77 K inner windows. Substrates pose a more serious problem; the in-plane index difference in the terahertz range is 0.3 for $(1\bar{1}02)$ oriented sapphire. The waveplate-like effect of the substrate is largely eliminated by aligning the incident polarization to within 1° of its optical axis, thus ensuring that the polarization incident on the film is remains linear. Taking the above precautions typically yields an extinction ratio of 25.

The experimental procedure for measuring t_{xy} due to Faraday rotation is as follows: At each temperature and magnetic field, both $t_{xy}(\omega)$ and $t_{xx}(\omega)$ are measured and the substrate phase shift $\Phi(\omega)$ is canceled in the ratio t_{xy}/t_{xx}. To eliminate the effect of linear birefringence we take advantage of the unique field dependence of the magneto-optic effects we seek to measure. The Faraday effect is an odd function of the magnetic field while the signal due to birefringence is even. The spurious component of t_{xy}/t_{xx} measured at positive field can be removed by subtracting that measured at negative field. This procedure was checked using a bare substrate in place of the sample. The rotation was less than 2×10^{-4} radians for a 3 mm thick sapphire substrate and 8×10^{-4} radians for a 0.5 mm thick $LaAlO_3$ substrate.

The measurements were performed on three *in situ* $YBa_2Cu_3O_7$ films. Sample A (T_c = 84 K) is a 70 nm film grown by off-axis sputtering on a sapphire substrate with a CeO_2 buffer layer. Sample B (T_c = 88 K) is a 40 nm film grown by the same method, but on $LaAlO_3$. Sample C (T_c = 86 K) is 80 nm thick, and was grown by laser ablation on $LaAlO_3$. Results obtained for each of these films were qualitatively the same.

The complex Faraday effect t_{xy}/t_{xx} in film A at 150 GHz, in a magnetic field of 6 T, is shown in Figure 2. The real part corresponds to the rotation of the plane of polarization, and the imaginary part represents the amount of magnetically induced ellipticity in the transmitted light. Above T_c, t_{xy}/t_{xx} is real and varies approximately as $1/T^2$. This behavior is nothing more than the normal state Hall effect, as can be seen from the relation

$$\frac{t_{xy}}{t_{xx}} = \frac{Z_0 d\,\sigma_{xy}}{Z_0 d\,\sigma_{xx} + n + 1} \approx \frac{\sigma_{xy}}{\sigma_{xx}} = \tan(\theta_H), \quad (2)$$

where θ_H is the Hall angle. The approximation, which is not made in later analysis, is accurate because the film impedance is much less than Z_0 (377 Ω). The Hall angle at high frequency agrees quantitatively with the dc Hall effect in the normal state [6] because 150 GHz is far below the normal state scattering rate.

The structure near T_c, including the sign change of $\mathrm{Re}(t_{xy}/t_{xx})$, is also consistent with low frequency measurements [7] and has been attributed to vortex motion [8]. However, at still lower T our results differ from expectations based on dc measurements. At temperatures 10-15 K below T_c the low-frequency dissipation and Hall voltage become unmeasurably small due to freezing out of vortex motion, while at 150 GHz $\mathrm{Re}(t_{xy}/t_{xx})$ reverses sign again, increases to a positive maximum near 40 K, and tends to zero as T approaches zero. This contrast suggests that the Faraday rotation is unrelated to vortex dynamics over a broad range of temperature below T_c. The peak at 40 K implies that the magneto-optic response may be dominated instead by the damped cyclotron motion of quasiparticles.

To test this hypothesis we focus on the Faraday effect due to quasiparticle motion. We extend the conventional two-fluid model, assuming that in the presence of a magnetic field the conductivity tensor may be written as a sum of condensate and quasiparticle contributions [9]:

$$\tilde{\sigma} = \tilde{\sigma}_s + \tilde{\sigma}_n \approx \begin{bmatrix} \sigma_s & 0 \\ 0 & \sigma_s \end{bmatrix} + \begin{bmatrix} \sigma_n & \sigma_{xy} \\ -\sigma_{xy} & \sigma_n \end{bmatrix}. \quad (3)$$

Applying conventional transport theory, with a momentum and energy independent scattering rate, leads to the following off-diagonal component:

$$\frac{\sigma_{xy}(\omega)}{\sigma_0} = \frac{n_q}{n_0} \cdot \frac{\Gamma_0}{\Gamma} \cdot \frac{\omega_c/\Gamma}{(1 - i\omega/\Gamma)^2 + (\omega_c/\Gamma)^2}, \quad (4)$$

where σ_0, n_0, and Γ_0 are the dc conductivity, carrier density and scattering rate in the normal state, and $\omega_c = eB/m^*c$.

Calculating $\sigma_{xy}(\omega)$ requires knowledge of the quasiparticle density n_q, scattering rate Γ, and cyclotron frequency ω_c, as a function of the temperature. We estimate the first two parameters by analyzing the complex zero-field conductivity measured on the same series of samples. Again using a Drude model for the quasiparticle dynamics [10], we find a normalized conductivity

$$\frac{\sigma}{\sigma_0} = \frac{\sigma_s + \sigma_q}{\sigma_0} = \frac{i n_s \Gamma_0}{n_0 \omega} + \frac{n_q}{n_0} \frac{\Gamma_0}{(\Gamma - i\omega)}, \quad (5)$$

where $n_q + n_s = n_0$. The main panel of Fig. 3 compares a plot of Eq. (5), using $n_q(T)$ and $\Gamma(T)$ shown in the inset, to the measured real part of the conductivity σ_1 at 250 GHz. The functions $n_q(T)$ and $\Gamma(T)$ were inferred from the data subject to the constraints that $n_q(0) = 0$ and that Γ decrease monotonically with decreasing T, approaching a constant at low temperature. As is now widely accepted, the rise in σ_1 from T_c to 40 K, which takes place in spite of a diminishing n_q, is caused by a rapid decrease in Γ. The drop in σ_1 at 250 GHz below 40 K indicates either that Γ has swept below the measurement frequency or that it has reached a temperature independent elastic scattering rate Γ_{el}. In our thin film samples the drop in σ_1 at 100 GHz occurs at the same T, indicating that Γ_{el} is reached at ~40 K.

The quasiparticle density and scattering rate shown in Fig. 3 reproduce the trends in zero-field conductivity for all three samples over our entire frequency range from 100-800 GHz. We next use the same $n_q(T)$ and $\Gamma(T)$ as input to Eq. (4) to estimate the quasiparticle contribution to $\sigma_{xy}(\omega)$. The cyclotron frequency was chosen to be

40 GHz at 6 T, corresponding to a temperature independent effective mass of $4m_e$.

Figure 4 compares the predictions of Eq. (4) with the real and imaginary parts of σ_{xy} as calculated from the transmission tensor. The data for sample B are shown because they cover the widest frequency range; the other two samples showed similar behavior. In each panel we plot σ_{xy} *vs.* T for several frequencies between 150 and 800 GHz. Referring first to the 150 GHz curves, one immediately notices that the model predicts a peak at 40 K in both the real and imaginary parts of σ_{xy} which is mirrored in the corresponding data. Most striking is the agreement in magnitude. The model and the data, which are both normalized to σ_0 at 100 K, agree to within about 50% at the peaks; both the real and imaginary parts appear to exceed the prediction by a factor of ~1.5.

The model curves change dramatically as ω increases from 150 to 800 GHz because $\Gamma(T)$ inferred from the zero-field conductivity sweeps through this range. In fact Re $\sigma_{xy}(T)$ is much more sensitive to Γ than $\sigma_1(T)$; its shape evolves from a peak to a zero-crossing at 40 K as frequency increases. Again, the experimental results display the same trends as the model, implicating damped cyclotron motion of quasiparticles as the origin of the Hall effect over a broad range of temperature in the superconducting state.

Significant deviations between the model and experiment do appear, however, at the lowest temperatures at which measurements were performed. Of course the model predicts that $\sigma_{xy}(T)$ tends to zero as we have assumed the quasiparticle density vanishes at $T = 0$. In contrast, both real and imaginary parts of the measured $\sigma_{xy}(T)$ appear to approach a non-zero asymptote as T tends to zero. One possible explanation is that as quasiparticles disappear into the condensate, the vortex contribution, masked at higher temperatures, begins to show through. Indeed, Choi *et al.* [11] have reported magneto-optic activity at 2 K in thin films of $YBa_2Cu_3O_7$ and interpreted the Faraday rotation in terms of vortex dynamics. Recent theoretical studies [12] of quasiparticle conductivity in the presence of disorder suggest another possibility. If a perfect $YBa_2Cu_3O_7$ crystal retains lines of the Fermi surface in the superconducting state, then disorder, clearly present in thin films, may induce finite areas of Fermi surface. In this picture the density of quasiparticles remains non-zero at $T = 0$, although their contribution to the Hall effect has yet to be calculated.

In addition to understanding the Faraday effect better at the lowest temperatures, other important questions remain to be addressed. For example, will the Faraday rotation be significantly greater in samples with smaller Γ_{el}, as our model would predict? Second, the temperature dependence of the dc Hall angle [6] implies that the scattering rate for cyclotron motion differs from the transport scattering rate. Does this distinction extend to the superconducting state? The agreement in magnitude between model and experiment discussed earlier suggests that conventional dynamics describes the cyclotron motion in the superconducting state. However, this reasoning is based on the untested assumption that Γ is not strongly affected by a 6 T field. Future work will address these issues, focusing on the conductivity tensor as an additional probe of quasiparticle dynamics in the superconducting state.

This work was supported under NSF Grant No. FD92-04394. We are also grateful to the Director, Office of Basic Energy Sciences, Department of Energy under Contract No. DE-AC03-76SF00098, the University of California, Berkeley, and the AT&T Foundation for instrumentation funding. S.S. acknowledges the sup-

port of the Miller Institute for Basic Research in Science.

References

[1] M.C. Nuss *et al.*, Phys. Rev. Lett. **66**, 3305 (1991).

[2] D.A. Bonn *et al.*, Phys. Rev. Lett. **68**, 2390 (1992).

[3] W.N. Hardy *et al.*, Phys. Rev. Lett. **70**, 399 (1993).

[4] P.B. Miller, Phys. Rev. **121**, 445 (1961).

[5] D.H. Auston, in *Ultrashort Laser Pulses and Applications, Springer Topics in Applied Physics*, **60**, edited by W. Kaiser (Springer-Verlag, Berlin, 1988).

[6] N.P. Ong, in *Physical Properties of High Temperature Superconductors II,* edited by D.M. Ginsberg (World Scientific, Singapore, 1990).

[7] Y. Iye *et al.*, Physica (Amsterdam) **159C**, 616 (1989); M. Galffy *et al.*, Solid State Commun. **68**, 929 (1988).

[8] S.J. Hagen *et al.*, Phys. Rev. B **41**, 11630 (1993); J.M. Harris *et al.*, Phys. Rev. Lett. **71**, 1455 (1993).

[9] In Eq. (3) we ignore the off-diagonal contribution of the condensate. As explained in T. Hsu, Physica C **213**, 305 (1993), while a translationally invariant superconductor at $T = 0$ would exhibit a large σ_{xy}, vortex pinning reduces the off-diagonal conductivity of the superfluid condensate. In our model we test the assumption that the pinning is sufficiently strong that the quasiparticle contribution dominates $\sigma_{xy}(\omega)$.

[10] D.A. Bonn *et al.*, Phys. Rev. B **47**, 11314 (1993).

[11] E. Choi, *et al.* (to be published).

[12] P.J. Hirschfeld *et al.*, Phys. Rev. Lett. **71**, 3705 (1993); P.A. Lee, Phys. Rev. Lett. **71**, 1887 (1993).

Figure Captions

Fig. 1: Time-domain spectrometer for measurement of the complex transmission tensor in the presence of a magnetic field. Diagonal t_{xx} and off-diagonal t_{xy} components are selected by rotating the analyzing polarizer through 90°. The effect of linear birefringence is removed by reversing the field direction.

Fig. 2: Real and imaginary parts of the ratio of the off-diagonal to diagonal transmission, t_{xy}/t_{xx}, a quantity which is related to the Hall angle, measured at 150 GHz. $\mathrm{Re}(t_{xy}/t_{xx})$ follows the dc Hall effect above and near T_c, but rises to maximum near 40 K, at which temperature the dc Hall effect has become unmeasurably small.

Fig. 3: Real part of the conductivity σ_1 at 250 GHz measured in zero magnetic field, as a function of the temperature. The inset shows the quasiparticle density $n_q(T)$ and momentum relaxation rate $\Gamma(T)$ inferred from the complex $\sigma(T)$ at 250 GHz by assuming a Drude model for the quasiparticle conductivity. $\sigma_1(T)$ corresponding to these parameters is plotted as a solid line in the main panel.

Fig. 4: (a) Conventional transport model and (b) experimentally determined real and imaginary parts of σ_{xy} as a function of temperature for several frequencies between 150 and 800 GHz. The input parameters to the model are the quasiparticle density and momentum relaxation rate consistent with the zero-field conductivity (see Fig. 3 inset). The cyclotron frequency was chosen to be 40 GHz, corresponding to an effective mass of $4m_e$ and a field of 6 T.

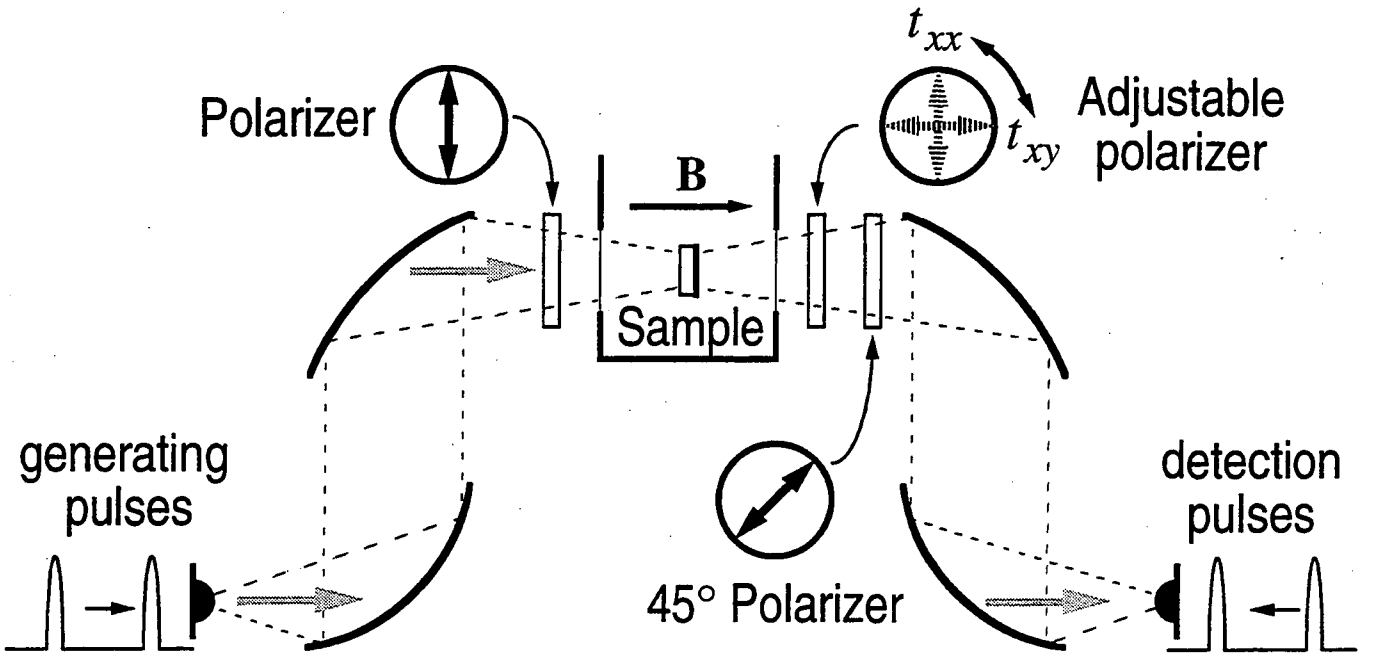

Figure 1

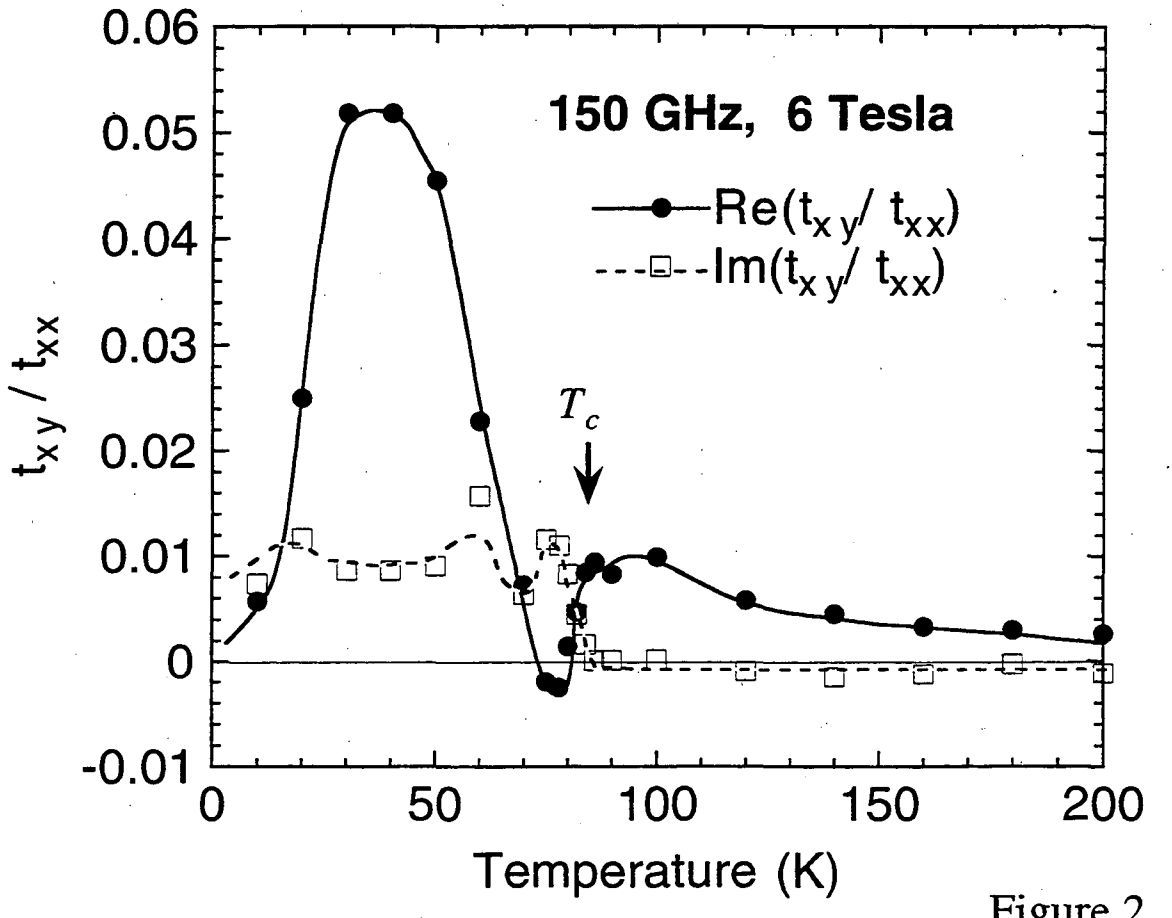

Figure 2

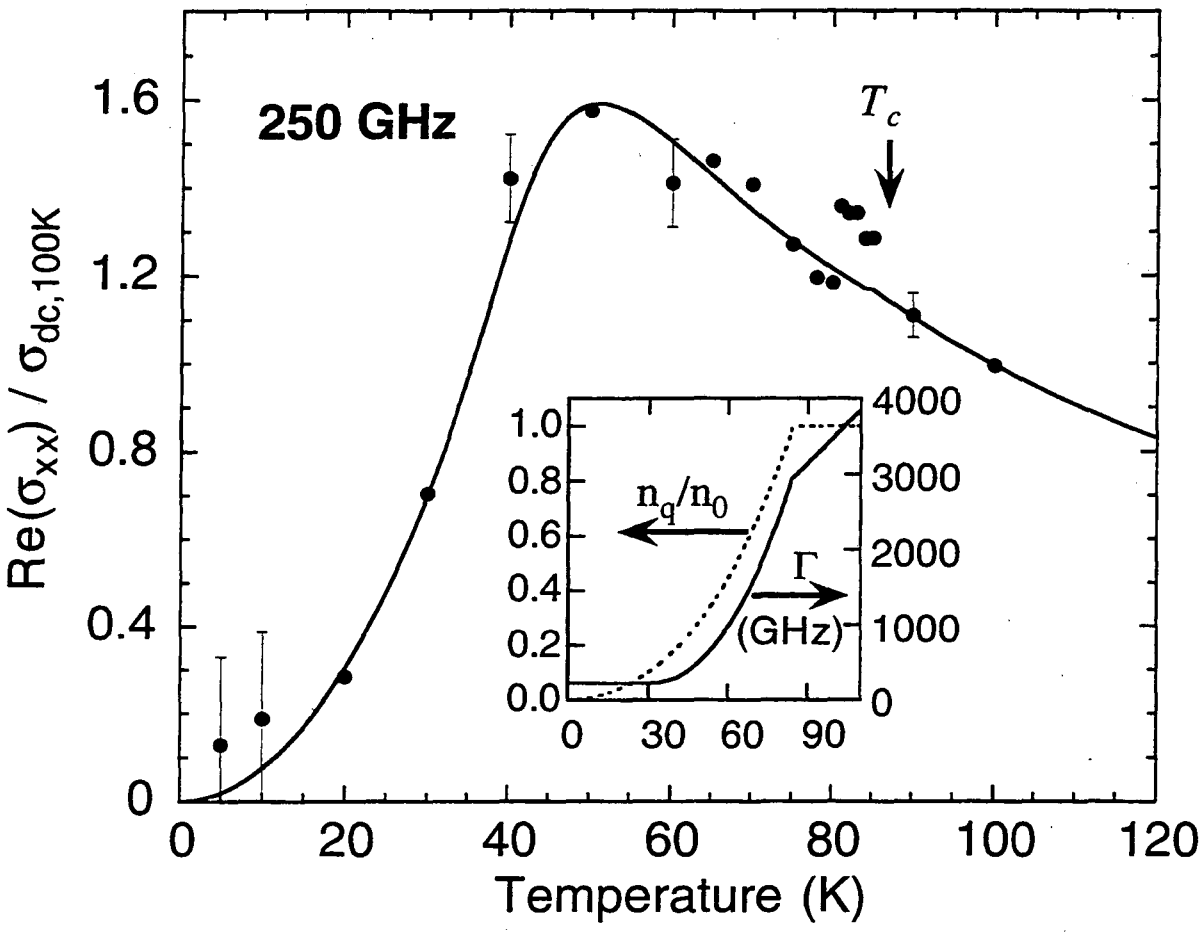
250 GHz
T_c
$\mathrm{Re}(\sigma_{xx}) / \sigma_{dc,100K}$
Temperature (K)
n_q/n_0
Γ
(GHz)

Figure 3

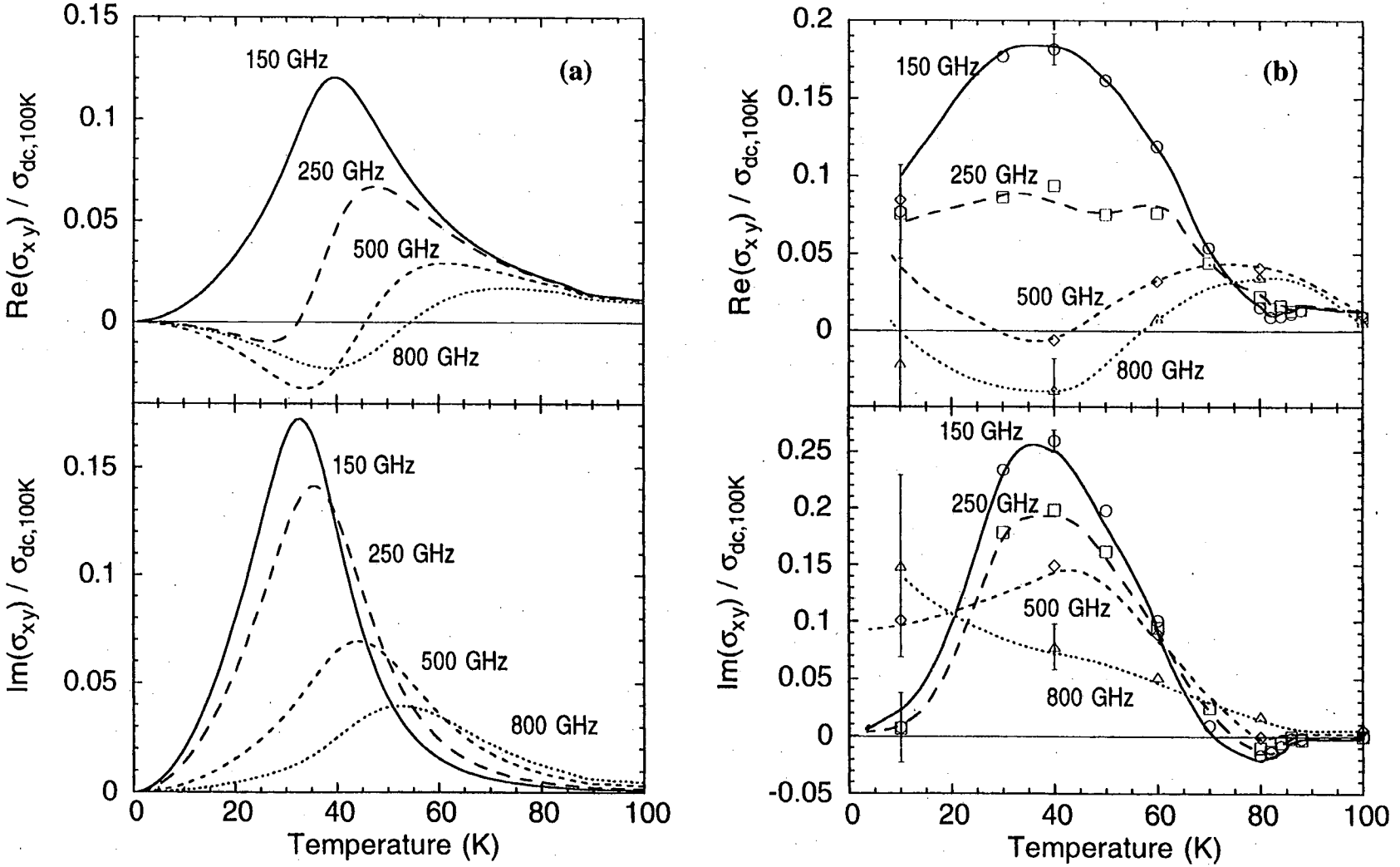
(a)
(b)
150 GHz
250 GHz
500 GHz
800 GHz
Re(σxy) / σdc,100K
Im(σxy) / σdc,100K
Temperature (K)
0.15
0.1
0.05
0
0.2
0.25
-0.05
0
20
40
60
80
100

Figure 4

LAWRENCE BERKELEY LABORATORY
UNIVERSITY OF CALIFORNIA
TECHNICAL INFORMATION DEPARTMENT
BERKELEY, CALIFORNIA 94720